


## ORIGINAL RESEARCH

# A lane changing time point and path tracking framework for autonomous ground vehicle

Jiayu Fan  | Jun Liang | Anjan K. Tula

The State Key Lab of Industrial Control  
Technology, Zhejiang University, Hangzhou, China

**Correspondence**

Jun Liang, The State Key Lab of Industrial Control  
Technology, Zhejiang University, Hangzhou 310027,  
China.

Email: jliang@zju.edu.cn

**Funding information**

National Key R&D Program of China,  
Grant/Award Number: 2019YFB1600500; National  
Natural Science Foundation of China, Grant/Award  
Number: U1664264

**Abstract**

Performing stable and safe lane changes can avoid collisions and improve traffic safety. In recent years, most of the research in automated ground transportation was focused on path planning and path tracking. However, this work emphasizes the importance of lane changing time point. Based on traditional safety distance, a novel concept, that is the synthesized safety distance for lane changing (SSDLC), is proposed to study lane changing time point. It consists of the reference safety distance and lane changing safety distance, and the weight coefficient between them is obtained by fuzzy logic control algorithm. Additionally, the joint model predictive control (JMPC) is proposed to follow the reference trajectory. This newly established algorithm not only considers the physical saturation of actuators but the yaw stability characteristics. To overcome the calculation difficulty to obtain the optimal results in the prescribed time, the algorithm adds a relaxation factor in the objective function. Finally, the lane changing time point and path tracking framework is modeled and simulated on a CarSim-Simulink platform. Four scenarios are carried out to illustrate the feasibility of the proposed framework.

## 1 | INTRODUCTION

In recent years, the traffic accidents resulting from people frequently happen. In order to reduce these accidents and improve car driving safety, autonomous ground vehicle (AGV) is brought to the forefront. Every AGV is equipped with many active safety systems which can ensure vehicle safety and stability. Among these, the active vehicle collision avoidance system is one crucial portion, which conducts lane changing behavior by means of previous path planning and tracking. When the intelligent vehicle receives the collisions information (dynamic or static) from sensors and cameras, the vehicle control unit (VCU) formulates the lane changing maneuver, generating the collision-free path and commanding the controller to tracking the planned path.

The common path planning algorithms include potential fields, cell decomposition, interdisciplinary methods and optimal control [1, 2]. Potential field algorithms assign repulsive fields to obstacles and attractive fields to target points and then use an algorithm to compute trajectories along the steepest potential gradient in the resulting field. However, this

approach has limitations in handling system constraints and its computation cost is also high [3]. Cell decomposition algorithms such as Rapidly-exploring Random Tree (RRT) [4] is an effective method used for collision-free path planning. These algorithms can be modified to incorporate the vehicle constraints, but they also suffer from computational and memory costs. Optimal control methods minimize a performance index (change in kinetic energy, jerk, lateral acceleration) under a set of constraints (vehicle lateral, longitudinal limits, environment constraints, neighboring vehicles) to obtain a trajectory for a safe overtaking maneuver. The results from literature demonstrate that the method is successful in generating collision free trajectories without high computational requirements. Based on optimal control theory, some researchers propose a novel method to model the trajectories of vehicles in two-dimensional space and speed, which achieves good results [5]. Other researchers [6] minimize the trip time by use of Pontryagin's minimum principle and they also get an 80% reduction in delay. However, optimal method cannot be applied for high speed driving maneuver with large angles of tire slip [7].

This is an open access article under the terms of the [Creative Commons Attribution-NonCommercial-NoDerivs](https://creativecommons.org/licenses/by-nc-nd/4.0/) License, which permits use and distribution in any medium, provided the original work is properly cited, the use is non-commercial and no modifications or adaptations are made.

© 2022 The Authors. *IET Intelligent Transport Systems* published by John Wiley & Sons Ltd on behalf of The Institution of Engineering and Technology.

A successful lane changing maneuver does not end with just path planning but extends to make the strategy that control the actuator of the vehicle to track the generated trajectory. Many tracking algorithms have been proposed for the conventional vehicle handling and stability control, such as fuzzy control algorithm [8], robust control [9], output-feedback control algorithm [10], learning control algorithm [11, 12], model predictive control (MPC) [13] etc. Some researchers employ a supertwisting second-order sliding mode control strategy and the result shows that this technique obtains less tracking error [14]. Among these methods, the MPC algorithm is an effective method to tackle multiple constrained questions. Some researchers use MPC to solve optimization problem by treating the lateral velocity of vehicle at the end point of the lane change as an intermediate variable and through this way they achieve acceptable obstacle avoidance performance [15]. So MPC has the provision of inclusion of constraints in computation of the optimal solution, which makes MPC preferred over other methods.

Although there has been substantial research on path planning and tracking in collision avoidance system for AGV [16], many aspects on lane changing still need to be investigated, more specifically, on lane changing time point. As a matter of fact, when driver driving the car comes across an obstacle in front of the road, if he would conduct lane changing maneuver, he first judges the appropriate lane changing time point based on experience. When already overtaking the obstacle in the adjacent lane, he also judges the appropriate time point to return to the original lane based on experience. Changing the lane in the appropriate time point can ensure the yaw stability, avoid the risk of collision and improve the efficiency of lane changing and obstacle avoidance. It also leaves the enough room for planning the path. Apart from this, many of path tracking algorithms just consider the saturation limits of the vehicle's actuators [4], [17]. In fact, when the car changing the lane, the dynamic nonlinear characteristics of vehicle, that is the yaw stability, also need to be considered.

This paper describes an novel approach for lane changing time point. The synthesized safety distance for lane changing (SSDLC) is firstly proposed to describe the lane changing time point. It is defined as the weighted sum of traditional safety distance and lane changing safety distance. Regard the velocity information of the ego vehicle and the surrounding vehicles as the input and the weight of the mentioned safety distance as the output. And the SSDLC is calculated by fuzzy logic control algorithm. After obtaining the appropriate lane changing time point, the whole lane changing process will begin. In path tracking aspect, the joint model predictive control (JMPC) with multiple constraints is proposed to follow the reference trajectory. This algorithm not only considers the physical saturation of actuators of the vehicle, but the nonlinear stability characteristics of lane changing condition are also included. At the same time, the JMPC adds a relaxation factor in the objective function to obtain the optimal results in the prescribed time.

## 2 | ANALYSIS OF LANE CHANGING PROCESS

At present, highway roads, urban trunk roads and other roads belong to structured roads [18]. Such roads have clear marking lines, single background environment and obvious geometric characteristics. In the structured road, the road lines are the main determinant of the road, so the road detection problem can be simplified to the detection of the lane lines and road boundary. Equipped sensors such as cameras only need to identify the road boundary, the lane lines and obstacles and these are enough to meet the basic task of perception.

This paper studies the task of changing lanes and avoiding obstacles on structured roads. The vehicle moves straight along the centerline of the lane when driving normally, and drives along the planned trajectory to the centerline of the adjacent lane when performing the task of changing lanes and avoiding obstacles. After completing the task of overtaking (dynamic obstacles such as cars) and obstacle avoidance (static obstacles such as rocks) along the centerline of adjacent lanes, return to the centerline of the original lane along the planned trajectory. And then the entire lane changing and obstacle avoidance task complete.

The workflow of the lane changing process is as following: When the intelligent vehicle comes across obstacles in the current driving road, the entire process of obstacle avoidance is analyzed according to driving behavior habits. First of all, the intelligent vehicle environment perception unit understands the driving intentions of surrounding vehicles and obtains information about obstacles through sensors and V2X interconnection communication. These information includes the speed of ego vehicle, relative speed and relative distance between ego vehicle and leading vehicle. Then, the decision-making unit determines the time point of changing lanes based on fuzzy logic algorithm. After that, the starting point can be decided. Next the planning unit will plan a safe, stable and effective path based on sine curve method. Finally the control execution unit applies JMPC algorithm to track the generated path in real time, outputting speed and steering angle of ego vehicle to conduct the lane changing mission. The whole research framework is shown in Figure 1.

### 2.1 | Research on the lane changing time point

#### 2.1.1 | The definition of the synthesized safety distance for lane changing

The lane changing time point is related to the relative distance of the front and the rear vehicle. So the safety distance is studied to describe the lane changing time point. However, the safe distance between the intelligent vehicle and its front vehicle cannot be the same as the distance between the manned vehicle and its front vehicle. When the driver is driving, due to the consideration of the driver's reaction time and the actuators'

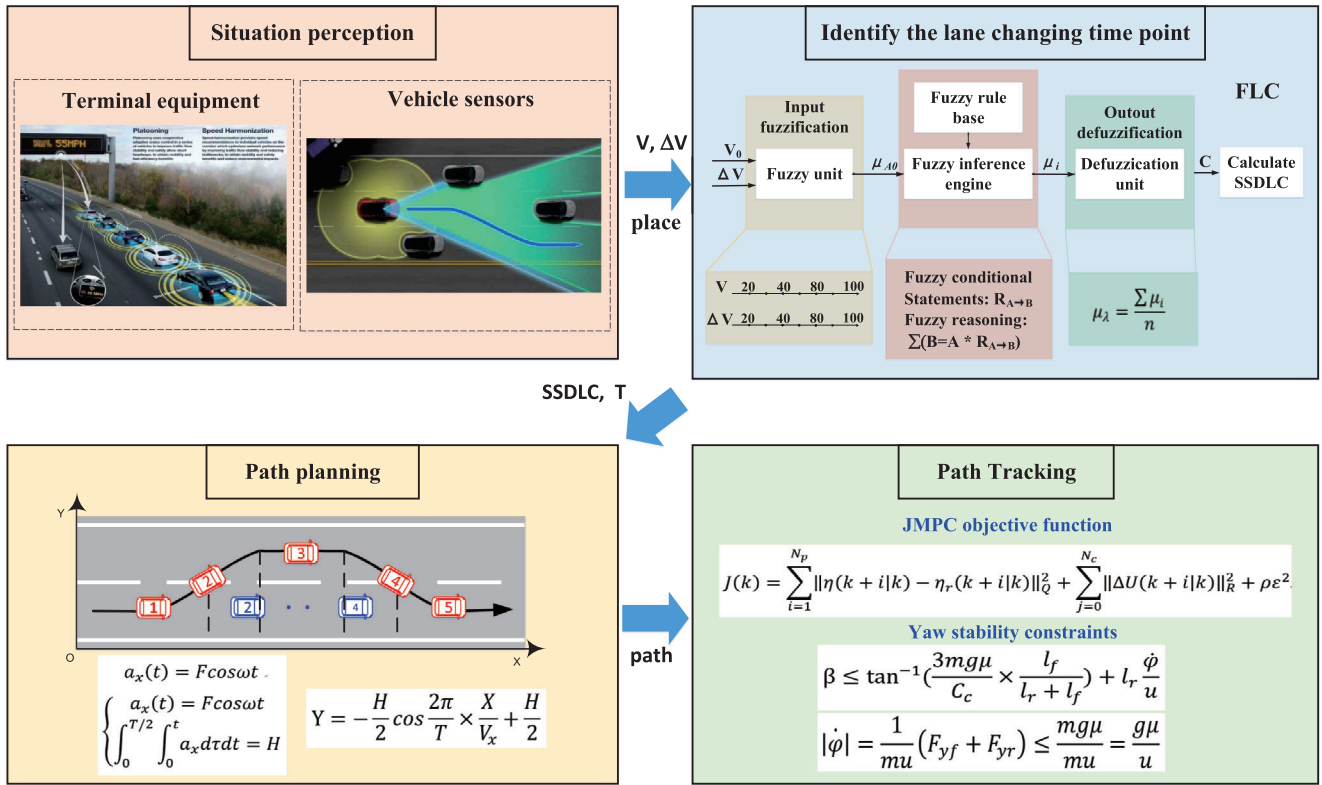


FIGURE 1 The lane changing research framework

effect time, the safe distance regulated by traffic laws is relatively conservative. However, with the development of the level of vehicle intelligence, the vehicle is equipped with high computing capacity VCU and advanced wire control technology. These advanced technologies can greatly reduce the reaction time and the delay time of executing commands, and the prescribed safe distance should be adjusted accordingly. Such changes save road resources, improve the utilization rate of the road and increase the magnitude capacity of vehicles on the road.

The lane changing safety distance is essentially different from the traditional safe distance regulated by the toad traffic safety law. The lane changing safety distance is related to the relative speed of the front and rear vehicles, the speed of ego the vehicle, and the lane changing duration. The traditional safety distance is related to the speed of the vehicle and the braking time. The latter must meet this condition no matter what motion state of the front obstacle is in, so the traditional safety distance is relatively conservative. Each of these two kinds of distances cannot be integrated enough to describe the lane changing time point. One new kind of safety distance which can describe the lane changing time point needs to be studied.

The synthesized safety distance for lane changing (SSDLC) is first proposed to describe the lane changing time point. It is defined as the weighted sum of traditional safety distance and lane changing safety distance.

This article establishes the relationship between the two influence factors (the relative speed and lane changing duration) and the lane changing safety distance. Formulate the expression for calculating the lane changing safety distance. As for the impact

TABLE 1 The reference safety distance by Chinese traffic laws

Velocity level	Quantified velocity (km/h)	Safety distance (SD)(m)
Level I	$v \geq 100$	$SD > 100$
Level II	$100 > v \geq 60$	$SD = \text{size of } v$
Level III	$v \approx 50$	$SD > 50$
Level IV	$v < 40$	$SD > 30$
Level V	$v < 20$	$SD \geq 10$

of the speed of the ego vehicle on the lane changing safety distance, refer to the reference safety distance between vehicles regulated by traffic laws in Table 1. The prescribed safety distance considers both the speed and braking time of the vehicle, including the impact the speed of the ego vehicle on the lane changing safety distance. Finally, assigning weights to these two safety distances by fuzzy logic control algorithm, the SSDLC is obtained.

The formula of calculating lane changing safety distance is:

$$\begin{aligned} x_0 = & (V_0 - V_1)t + \int_0^t \int_0^\tau a_0(\tau) d\tau dt - \int_0^t \int_0^\tau a_1(\tau) d\tau dt \\ & + L_1 + L_2, \end{aligned} \quad (1)$$

where  $V_0$  and  $V_1$  are for the speed of ego vehicle and the speed of the heading vehicle, respectively.  $a_0$  and  $a_1$  are for the

acceleration of ego vehicle and the acceleration of the heading vehicle, respectively.  $L_1$  and  $L_2$  are car body length.

According to “Regulation on the Implementation of the Road Traffic Safety Law of the People’s Republic of China”, the traditional safety distance standard is given in Table 1.

Use a linear function to fit the relationship between vehicle speed and the reference safety distance:

$$SD = a * V + b, \quad (2)$$

where SD is safety distance, a and b are the coefficients of the linear function. The relative speed, the speed of the ego vehicle and lane changing duration all have a great impact on the SSDLC. The impact of lane change duration on lane changing safety is rarely considered. In theory, during the actual process of changing lanes, changing lanes too quickly will make other obstacles too late to respond and prone to accidents; changing lanes too slowly will lead to long-term occupation of two lanes, which increases the probability of accidents. From the results of traffic data statistics, the lane changing duration is generally between 3 s and 10s, and the longest lane changing duration is generally no more than 9s [19]. In order to facilitate the study of the impact of vehicle speed on lane changing safety, this paper assumes that the lane changing duration is 5 s.

### 2.1.2 | Identify the lane changing time point using fuzzy logic control

Consider the impact of the vehicle speed on SSDLC. When the vehicle speed is low, the reference safety distance provided by the law is small, that is, the safety distance determined by the speed of the ego vehicle is small. Nevertheless, the lane changing safety distance related to the relative speed and lane changing duration is relatively large. In this situation, the latter weight in SSDLC should be increased; when the vehicle speed is high, the impulse of the driving vehicle will grow large. In order to avoid risks and decrease the damage degree of traffic collisions, the safety distance related to the speed of the ego vehicle should be as large as possible. Because of mainly focusing on the relative speed, the lane changing safety distance related to the relative speed and lane changing duration is small. In this situation, the former weight in SSDLC should be increased.

In addition, the relative speed will also have a great impact on the weight of SSDLC. When the speed difference is large, rear-end collisions are prone to occur. In this situation, the lane changing safety distance is relatively large, and the weight in this factor should be increased; When the speed difference is small, the lane changing safety distance considering the relative speed and lane changing duration is small, and the contribution to SSDLC is limited. Therefore, the weight of the reference safety distance regulated by the traffic laws should be increased. For this kind of decision-making issue that tends to get results based on certain factors, this paper uses fuzzy logic control algorithms to formulate a comprehensive control strategy for the weight coefficient of SSDLC [20].

**TABLE 2** The rule base of fuzzy transformation

Fuzzy language results		Relative speed $\Delta V$ level		
		level S	level Z	level B
Speed $V_0$ level	level L	F7	F8	F9
	level M	F4	F5	F6
	level H	F1	F2	F3

The SSDLC consists of the lane changing safety distance and the reference safety distance, but the weight between the two needs to be allocated reasonably. The weight coefficient is related to the vehicle speed and the relative speed, so this paper designs a dual-input and single-output fuzzy logic controller with the vehicle speed and relative speed as input and weight coefficient as output. Accurate input is converted into fuzzy language variables through the fuzzification process. The control rules are set by experts. The fuzzification process is: write conditional sentences, confirm fuzzy relationship matrix, perform fuzzy mathematical calculations, and obtain language inference results. Finally, the results are converted into output value by defuzzification [21–23].

This paper takes the vehicle speed  $V_0$  and relative speed  $\Delta V$  in real-time state as input variables, takes the weight C of the lane changing safety distance  $d_{change}$  as the output variable, and then an adaptive fuzzy logic controller is designed. So the reference safety distance  $d_{refer}$  takes up (1-C) in SSDLC. The final expected SSDLC is expressed as:

$$D = C * d_{change} + (1 - C) * d_{refer}. \quad (3)$$

According to experience, select the domain of the first input variable  $V_0$  as [20, 40, 80, 100], and the fuzzy language is defined as L, M, H, respectively, for the low speed, medium speed, and high speed. Select the domain of the second input variable  $\Delta V$  as [20, 40, 80, 100], and the fuzzy language is defined as {S, Z, B}, respectively, for small, medium, large. Select the domain of the output variable weight coefficient C as [0, 0.1, 0.25, 0.35, 0.5, 0.65, 0.75, 0.9, 1], and the fuzzy language is defined as  $\{F_1, F_2, F_3, F_4, F_5, F_6, F_7, F_8, F_9\}$ , respectively, for extremely smaller, smaller, small, medium-small, medium, medium-large, large, larger, extremely larger. The rule base is Table 2.

## 2.2 | Path planning

The essence of path planning is to calculate a curve connecting the starting position and ending position. The requirement of path is that the curve should be continuous and smooth and the curvature should be bounded [24]. When changing lanes, the vehicle should turn the steering wheel continuously, and change the driving route lightly. The ideal lane changing process is that the lateral speed first increases and then decreases from the starting position to the adjacent lane centerline, and the lateral speed first increases reversely and then decreases from the adjacent lane centerline back to the original lane. At the same



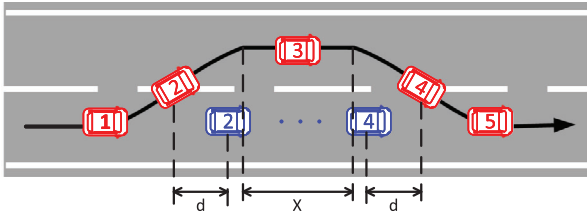


FIGURE 2 The lane changing procedure

time, the heading angle changes from 0 to the maximum, and then decreases to 0. This way of changing lanes can ensure that the lane changing curve is continuous and smooth, and the curvature is bounded. Also, the changing process is light, slow and stable, which can meet the constraints of vehicle dynamics.

At present, there are many kinds of lane-changing curves [25]. This paper selects the sine function curve that meets the aforementioned lane changing requirements. It has the advantages of minimum maximum trajectory curvature and smooth lane changing. From the above, we have determined the starting position of changing lane. In the geodetic coordinate system, the longitudinal speed of the vehicle will remain unchanged when changing lanes, plus knowing the lane change duration ( $T_L = 5s$ ), so the ordinate of the end position of changing lane can be calculated. According to the prescribed rule, the end position should end on the centerline of the adjacent lane, so that the abscissa of the end position can be also obtained. Up to now, the end position of changing lane can be determined. The starting position and the ending position of changing lane are known, the lane changing sine curve will be calculated.

When the vehicle tends to go back to the original lane, the time point is also important. Figure 2 illustrates the lane changing process.

In this section, the importance of how long the ego vehicle should drive in the adjacent lane is discussed. The appropriate safety place back to original lane should be taken into consideration. In real condition, the ego vehicle in red drives faster than the obstacle vehicle in blue. When the ego vehicle arrives in label 2 place, there is no collision happening and their distance  $d$  is nearly the least. Based on it, if the ego drives back to the lane line, that is label 4 place, the distance between them is also set  $d$ , and in this condition, the ego vehicle being faster, the collision can be avoided. The ego vehicle can go back to the original lane safely. From label 2 to label 4, the relative displacement is  $2*d$ , so the driving distance on the adjacent lane, that is  $X$  value, can be calculated.

The lane changing path of the vehicle conforms to the characteristics of the sine function. Keeping the starting position as origin of coordinates, the longitudinal direction as the  $X$ -axis direction, the lateral direction as the  $Y$ -axis direction. the lateral acceleration of the vehicle during the lane changing process is:

$$a_x(t) = F * \cos \omega t, \quad \times \begin{cases} a_x(t) = F * \cos \omega t \\ \int_0^{\frac{T}{2}} \int_0^t a_x d\tau dt = H \end{cases}, \quad (4)$$

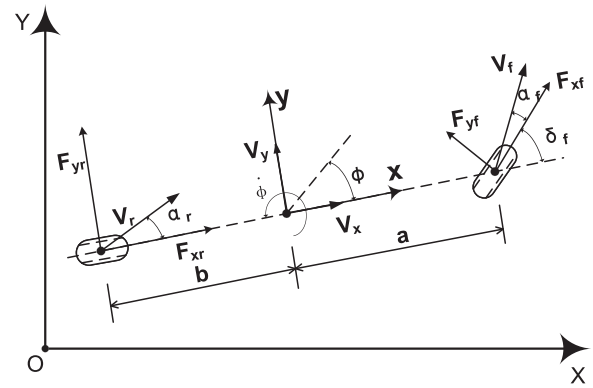


FIGURE 3 The vehicle dynamic model

where  $H$  is for the distance between the two adjacent centerlines,  $\omega = \frac{2\pi}{T_L}$ ,  $F = \frac{2\pi^2 H}{T_L^2}$ .

The lateral acceleration is integrated to obtain the lateral speed  $V_y$ , and  $V_y$  is integrated to obtain the lateral displacement  $Y$  during the lane changing process:

$$Y = -\frac{H}{2} \cos \frac{2\pi}{T_L} t + \frac{H}{2}. \quad (5)$$

During the lane changing process, the longitudinal speed keeps unchanged to ensure the ride fitness, set the speed as  $V_x$ ,

$$X = V_x * t. \quad (6)$$

Eliminate  $t$  by elimination method, the lane changing trajectory is:

$$Y = -\frac{H}{2} \cos \frac{2\pi}{T_L} \frac{X}{V_x} + \frac{H}{2}. \quad (7)$$

## 2.3 | Path tracking

### 2.3.1 | Constrains of vehicle dynamics considering yaw stability

This paper intends to select a three degree of freedoms(DOFs) vehicle dynamic model [19], considering the vehicle's lateral, longitudinal and yaw characteristics. The vehicle dynamic model is shown in Figure 3.

A few assumptions about vehicle model are:

1. Assume that the intelligent vehicle is driving along the lane centerline on a flat road, ignoring the vertical movement of the vehicle.
2. Assume that the suspension system and the vehicle are rigid, ignoring the suspension motion and its influence on the coupling relationship.
3. Assume that moment of inertia of vehicle model is constant and the barycenter cannot move for the lateral load transfer.

4. Assume the longitudinal speed keeps unchanged, the lateral acceleration  $a_y \leq 0.4g$  and the tire sideslip angle  $\alpha \leq 6^\circ$  during the lane changing.
5. Assume the wheelbase is negligible relative to the turning radius.
6. Ignore the influence of lateral and longitudinal aerodynamics on vehicle yaw characteristics.
7. Only consider the tire cornering characteristics, ignoring the coupling relationship of lateral and longitudinal tire forces.
8. Make a small angle hypothesis for the steering angle  $\delta$ ,  $\cos\delta \approx 1$ , and  $\sin\delta \approx \delta$ .

Carry out force analysis on the vehicle, and establish the dynamic equation of plane motion according to the force balance and moment balance of the vehicle:

$$\begin{cases} m(\dot{v}_x - V_y\dot{\phi}) = F_{xf}\cos\delta - F_{yf}\sin\delta + F_{xr} \\ m(\dot{v}_y - V_x\dot{\phi}) = F_{xf}\sin\delta + F_{yf}\cos\delta + F_{yr} \\ I_Z\ddot{\phi} = l_f(F_{xf}\sin\delta + F_{yf}\cos\delta) - l_rF_{tr} \\ \dot{X} = \dot{x}\cos\phi - \dot{y}\sin\phi \\ \dot{Y} = \dot{x}\sin\phi + \dot{y}\cos\phi \end{cases} \quad (8)$$

Set  $v_x = \dot{x}$ ,  $v_y = \dot{y}$ , change the form of the dynamic equation:

$$\begin{cases} \ddot{y} = -\dot{x}\dot{\phi} + \frac{2}{m} \left[ C_{cf} \left( \delta - \frac{\dot{y} + l_f\dot{\phi}}{v_x} \right) + C_{cr} \frac{l_r\dot{\phi} - \dot{y}}{\dot{x}} \right] \\ \ddot{x} = \dot{y}\dot{\phi} + \frac{2}{m} \left[ C_{lf}S_f + C_{cf} \left( \delta - \frac{v_y + l_f\dot{\phi}}{v_x} \right) \phi + C_{lf}S_r \right] \\ \ddot{\phi} = \frac{2}{I_Z} \left[ l_fC_{cf} \left( \delta - \frac{v_y + l_f\dot{\phi}}{v_x} \right) - l_rC_{cr} \frac{l_r\dot{\phi} - \dot{y}}{\dot{x}} \right] \\ \dot{X} = \dot{x}\cos\phi - \dot{y}\sin\phi \\ \dot{Y} = \dot{x}\sin\phi + \dot{y}\cos\phi \end{cases} \quad (9)$$

where  $m$  is the mass of the car,  $x$  and  $y$  are the longitudinal displacement and lateral displacement,  $v_x$  and  $v_y$  are the longitudinal speed and lateral speed,  $F_x$  and  $F_y$  are the longitudinal forces and lateral forces of tire,  $C_c$  and  $C_l$  are the cornering stiffness and longitudinal stiffness of tire.  $S_f$  and  $S_r$  are the longitudinal drift and lateral drift of tire.  $l_f$  and  $l_r$  are the distances of the front axis and the rear axis to the centroid.  $\phi$  is the yaw angle,  $\delta$  is the steering angle,  $I_z$  is inertia moment around the  $z$  axis [26].

When the longitudinal speed is constant or with a slow changing rate, the two DOFs vehicle dynamic model [9], [27] can be expressed as:

$$\begin{cases} \dot{\beta} = \frac{1}{m\mu} (F_{yf} + F_{yr}) - \dot{\phi} \\ \ddot{\phi} = \frac{1}{I_Z} (l_fF_{yf} - l_rF_{yr}) \end{cases} \quad (10)$$

where  $\beta$  is the vehicle sideslip angle. From the vehicle theory, when  $\dot{\beta}$  is close to 0, the vehicle dynamic state is stable, so the constraint of the yaw rate  $\dot{\phi}$  is :

$$|\dot{\phi}| = \frac{1}{mu} (F_{yf} + F_{yr}) \leq \frac{mg\mu}{mu} = \frac{g\mu}{u}, \quad (11)$$

where  $u$  is for the longitudinal speed and  $\mu$  is the attachment coefficient of road.

With a small angle hypothesis, considering the saturation characteristic of tire, the tire sideslip angle  $\alpha$  is stable on this condition:

$$\begin{aligned} \alpha &= \arctan \left( \beta - l_r \frac{\dot{\phi}}{u} \right) \approx \beta - l_r \frac{\dot{\phi}}{u} \\ &\leq \tan^{-1} \left( \frac{3mg\mu}{C_c} * \frac{l_f}{l_r + l_f} \right). \end{aligned} \quad (12)$$

So the constraint of the vehicle sideslip angle  $\beta$  [17] is :

$$\beta \leq \tan^{-1} \left( \frac{3mg\mu}{C_c} * \frac{l_f}{l_r + l_f} \right) + l_r \frac{\dot{\phi}}{u}. \quad (13)$$

### 2.3.2 | Path tracking using the joint model predictive control algorithm

The purpose of path tracking is to allow the intelligent vehicle to track a known reference path quickly and stably [28]. Model predictive control (MPC) has obvious advantages in dealing with high-dimensional, multi-variable, and constrained systems. The trajectory tracking controller designed by the MPC algorithm has better predictive ability on the future trajectory, and has a strong ability to deal with multi-objective constraints, so it has become a research hotspot [17]. This paper proposes the joint model predictive control (JMPC) with multiple constraints to follow the reference trajectory. This algorithm not only considers the physical saturation of actuators of the vehicle, but the non-linear stability characteristics of lane changing condition are also included. At the same time, the JMPC adds a relaxation factor in the objective function to solve the issue that obtain the optimal results in the prescribed time. Firstly, the predictive model should be established.

The vehicle tracking error model is one of common motion models in the path tracking field. Combined with the aforementioned two DOFs vehicle dynamic model, the predictive model can be expressed.

Suppose the lateral error as  $e_y$ , which is positive when the vehicle is on the left of path. Suppose the longitudinal error as  $e_x$ . Suppose the heading error as  $e_\phi$ , which is positive when in anticlockwise rotation. The turning radius is  $R$ . The expected yaw rate is:

$$\dot{\phi}_r = \frac{v_x}{R}. \quad (14)$$

The expected lateral acceleration is:

$$a_{yr} = v_x \dot{\phi}_r. \quad (15)$$

The lateral acceleration is:

$$a_y = \ddot{y} + v_x \dot{\phi}. \quad (16)$$

The lateral acceleration error is:

$$\ddot{e}_y = a_y - a_{yr} = \ddot{y} + v_x (\dot{\phi} - \dot{\phi}_r). \quad (17)$$

The lateral speed error is:

$$\dot{e}_y = \dot{y} + v_x (\phi - \phi_r). \quad (18)$$

The heading error is:

$$e_\phi = \phi - \phi_r. \quad (19)$$

The state variable  $X = [e_y, \dot{e}_y, e_\phi, \dot{e}_\phi, e_x, \dot{e}_x]^T$ , the control variable  $U = [\delta_f, a_e]^T$  represents the front steering angle and the longitudinal acceleration compensation, respectively. So the state function is:

$$\begin{aligned} \dot{X} &= A_e X + B_e U + \Gamma_e, \quad (20) \\ A_e &= \begin{bmatrix} 0 & 1 & 0 & 0 & 0 & 0 \\ 0 & -\frac{2C_{ef} + 2C_{er}}{mv_x} & \frac{2C_{ef} + 2C_{er}}{m} & 0 & 0 & 0 \\ 0 & 0 & 0 & 1 & 0 & 0 \\ 0 & -\frac{2C_{ef}a - 2C_{er}b}{I_Z v_x} & \frac{2C_{ef}a - 2C_{er}b}{I_Z} & 0 & 0 & 0 \\ 0 & 0 & 0 & 0 & 1 & 0 \\ 0 & 0 & 0 & 0 & 0 & 0 \end{bmatrix}, \\ B_e &= \begin{bmatrix} 0 & 0 \\ \frac{2C_{ef}}{m} & 0 \\ 0 & 0 \\ \frac{2C_{ef}a}{I_Z} & 0 \\ 0 & 0 \\ 0 & 1 \end{bmatrix}, \quad \Gamma_e = \begin{bmatrix} 0 \\ -\frac{2C_{ef}a - 2C_{er}b}{mv_x} - v_x \\ 0 \\ -\frac{2C_{ef}a^2 + 2C_{er}b^2}{I_Z v_x} \\ 0 \\ 1 \end{bmatrix} \dot{\phi}_r T_D. \end{aligned}$$

After the discretization, the state function will change into:

$$X(k+1) = AX(k) + BU(k) + \Gamma, \quad (21)$$

where  $A = I + A_e T_D$ ,  $B = B_e T_D$ ,  $\Gamma = \Gamma_e T_D$ :

$$\begin{aligned} B &= \begin{bmatrix} 0 & 0 \\ \frac{2C_{ef}}{m} T_D & 0 \\ 0 & 0 \\ \frac{2C_{ef}a}{I_Z} T_D & 0 \\ 0 & 0 \\ 0 & T_D \end{bmatrix}, \quad \Gamma = \begin{bmatrix} 0 \\ -\frac{2C_{ef}a - 2C_{er}b}{mv_x} - v_x \\ 0 \\ -\frac{2C_{ef}a^2 + 2C_{er}b^2}{I_Z v_x} \\ 0 \\ 1 \end{bmatrix} \dot{\phi}_r T_D \\ A &= \begin{bmatrix} 1 & T_D & 0 & 0 & 0 & 0 \\ 0 & 1 - \frac{2C_{ef} + 2C_{er}}{mv_x} T_D & \frac{2C_{ef} + 2C_{er}}{m} T_D & 0 & 0 & 0 \\ 0 & 0 & 0 & 1 & 0 & 0 \\ 0 & -\frac{2C_{ef}a - 2C_{er}b}{I_Z v_x} T_D & \frac{2C_{ef}a - 2C_{er}b}{I_Z} T_D & 0 & 0 & 0 \\ 0 & 0 & 0 & 0 & 1 & 0 \\ 0 & 0 & 0 & 0 & 0 & 1 \end{bmatrix} \end{aligned}$$

For the sake of the J MPC algorithms, establish a new state variable  $\xi(k|k)$ :

$$\xi(k|k) = \begin{bmatrix} x(k|k) \\ u(k-1|k) \end{bmatrix}$$

So the new state space function is:

$$\begin{cases} \xi(k+1|k) = \tilde{A}\xi(k|k) + \tilde{B}\Delta U(k|k) + \tilde{\Gamma} \\ \eta(k|k) = C\xi(k|k) \end{cases}, \quad (22)$$

where  $\tilde{A} = \begin{bmatrix} A & B \\ 0 & I \end{bmatrix}$ ,  $\tilde{B} = \begin{bmatrix} B \\ I \end{bmatrix}$ ,  $\tilde{\Gamma} = \begin{bmatrix} \Gamma \\ 0 \end{bmatrix}$ ,  $C = \begin{bmatrix} I \\ 0 \end{bmatrix}$ ,  $\Delta U(k|k) = U(k|k) - U(k-1|k)$ . Suppose the prediction horizon of the system is  $N_p$ , the control horizon is  $N_c$ . In the prediction horizon, calculate the state variables by the iteration of the state space function.

$$\xi(k+1|k) = \tilde{A}\xi(k|k) + \tilde{B}\Delta U(k|k) + \tilde{\Gamma}$$

$$\begin{aligned}
\xi(k+2|k) &= \tilde{A}^2 \xi(k|k) + \tilde{A} \tilde{B} \Delta U(k|k) \\
&\quad + \tilde{B} \Delta U(k+1|k) + \tilde{A} \tilde{\Gamma}(k) \\
&\quad + \tilde{\Gamma}(k+1) \\
&\quad \vdots \\
\xi(k+N_p|k) &= \tilde{A}^{N_p} \xi(k|k) + \tilde{A}^{N_p-1} \tilde{B} \Delta U(k|k) + \dots \\
&\quad + \tilde{A}^{N_p-N_c} \tilde{B} \Delta U(k+N_c-1|k) + \tilde{A}^{N_p-1} \tilde{\Gamma}(k) \\
&\quad + \tilde{A}^{N_p-2} \tilde{\Gamma}(k+1) + \dots + \tilde{\Gamma}(k+N_p-1)
\end{aligned}$$

Change the state variables into other forms. Set  $Y(k)$ ,  $\Delta U(k)$ ,  $U(k)$ ,  $\Omega(k)$  as:

$$\begin{cases}
Y(k) = [\eta(k+1|k), \eta(k+2|k) \dots \eta(k+N_p|k)]^T \\
\Delta U(k) = [\Delta U(k|k), \Delta U(k+1|k) \dots \Delta U(k+N_c-1|k)]^T \\
U(k) = [U(k|k), U(k+1|k) \dots U(k+N_c-1|k)]^T \\
\Omega(k) = [\tilde{\Gamma}(k|k), \tilde{\Gamma}(k+1|k) \dots \tilde{\Gamma}(k+N_p-1|k)]^T
\end{cases}$$

So the iteration process can be simplified as:

$$Y(k) = \Psi \xi(k|k) + \Theta(k) + \Pi \Omega(k)$$

$$\begin{aligned}
\Theta &= \begin{bmatrix} C\tilde{B} & 0 & \dots & 0 \\ C\tilde{A}\tilde{B} & C\tilde{B} & \dots & 0 \\ \vdots & \vdots & \ddots & \vdots \\ C\tilde{A}^{N_c-1}\tilde{B} & C\tilde{A}^{N_c-2}\tilde{B} & \dots & C\tilde{B} \\ \vdots & \vdots & \ddots & \vdots \\ C\tilde{A}^{N_p-1}\tilde{B} & C\tilde{A}^{N_p-2}\tilde{B} & \dots & C\tilde{A}^{N_p-N_c}\tilde{B} \end{bmatrix} \\
\Psi &= \begin{bmatrix} C\tilde{B} \\ C\tilde{A}^2 \\ \vdots \\ C\tilde{A}^{N_c-1} \\ \vdots \\ C\tilde{A}^{N_p-1} \end{bmatrix} \\
\Pi &= \begin{bmatrix} C & 0 & \dots & 0 \\ C\tilde{A} & C & \dots & 0 \\ \vdots & \vdots & \ddots & \vdots \\ C\tilde{A}^{N_p-1} & C\tilde{A}^{N_p-2} & \dots & C \end{bmatrix} \quad (23)
\end{aligned}$$

In order to achieve fast and stable tracking of the desired trajectory, an appropriate objective function needs to be established. According to the needs of the control system, the

objective function should not only optimize the system state, but also optimize the control increment to avoid the large change of the controller. And because of the complexity of dynamic model, it may happen that the optimal results can't be obtained within the prescribed time during the implementation process of controller. So objective function of the J MPC algorithm is defined as:

$$\begin{aligned}
J(k) &= \sum_{i=1}^{N_p} \|\eta(k+i|k) - \eta_r(k+i|k)\|_Q^2 \\
&\quad + \sum_{j=0}^{N_c} \|\Delta U(k+j|k)\|_R^2 + \rho \epsilon^2
\end{aligned} \quad (24)$$

And then the constraints of variables has to be considered. The proposed J MPC with multiple constrains either considers the physical saturation of actuators of the vehicle, or the nonlinear stability characteristics of lane changing condition are also included. The physical saturation of actuators is substituted by restricting control variable  $U$ , control increment  $\Delta U$ , state variable  $\eta$ . The nonlinear yaw stability is substituted by restricting vehicle sideslip angle  $\beta$ , and yaw rate  $\dot{\phi}$  [29].

The constrains of control variable  $U$ :

$$U_{min}(k+i) \leq U(k+i) \leq U_{max}(k+i)$$

The constraints of control increment  $\Delta U$ :

$$\begin{aligned}
\Delta U_{min}(k+i) &\leq \Delta U(k+i) \leq \Delta U_{max}(k+i) \\
(i &= 0, 1, \dots, N_c - 1)
\end{aligned}$$

The state constraints of state variable  $\eta$ :

$$\begin{aligned}
\eta_{min}(k+i) &\leq \eta(k+i) \leq \eta_{max}(k+i) \\
\times (i &= 0, 1, \dots, N_p)
\end{aligned}$$

The state constraints of vehicle sideslip angle  $\beta$  is:

$$\beta \leq \tan^{-1} \left( \frac{3mg\mu}{C_c} * \frac{l_f}{l_r + l_f} \right) + l_r \frac{\dot{\phi}}{u}$$

The state constraints of yaw rate  $\dot{\phi}$ :

$$|\dot{\phi}| = \frac{1}{mu} (F_{yf} + F_{yr}) \leq \frac{mg\mu}{mu} = \frac{g\mu}{u}$$

Then the objective function and the constraints are listed as programming question:

$$\begin{aligned}
min &= \sum_{i=1}^{N_p} \|\eta(k+i|k) - \eta_r(k+i|k)\|_Q^2 \\
&\quad + \sum_{j=0}^{N_c} \|\Delta U(k+j|k)\|_R^2 + \rho \epsilon^2,
\end{aligned} \quad (25)$$



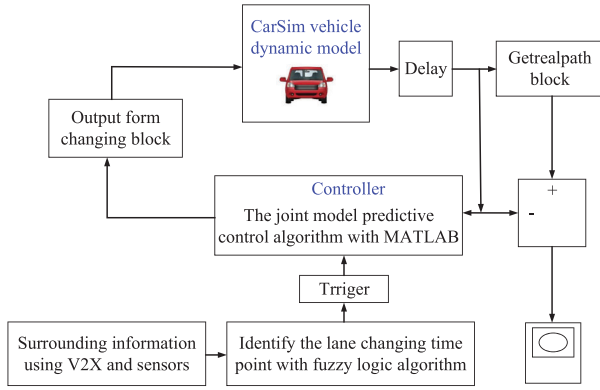


FIGURE 4 The established framework using simulation software

$$s.t. \begin{cases} U_{min}(k+i) \leq U(k+i) \leq U_{max}(k+i) \\ \Delta U_{min}(k+i) \leq \Delta U(k+i) \leq \Delta U_{max}(k+i) \\ U_{min}(k+i) \leq U(k-1) + \tilde{I}\Delta(k) \leq U_{max}(k+i) \\ \eta_{min}(k+i) \leq \eta(k+i) \leq \eta_{max}(k+i) \end{cases}$$

where

$$\tilde{I} = \begin{bmatrix} I & 0 & \cdots & 0 \\ I & I & \cdots & 0 \\ \vdots & \vdots & \ddots & \vdots \\ I & I & I & I \end{bmatrix}.$$

Suppose the reference output variable is:

$$Y_{ref}(k) = [\eta_{ref}(k+1|k), \eta_{ref}(k+2|k) \cdots \eta_{ref}(k+N_p|k)]^T$$

In the predictive horizon, the output error of the predictive model is defined as:  $E(k) = Y(k) - Y_k(k)$ , after some matrix calculations, the objective function is changed into standard quadratic form:

$$J(k) = \begin{bmatrix} \Delta(k) \\ \epsilon \end{bmatrix}^T H \begin{bmatrix} \Delta(k) \\ \epsilon \end{bmatrix} + G \begin{bmatrix} \Delta(k) \\ \epsilon \end{bmatrix} + P \quad (26)$$

Where

$$H = \begin{bmatrix} \Theta^T Q \Theta & 0 \\ 0 & \rho \end{bmatrix},$$

$$G = [2E^T(k)Q\Theta \quad 0],$$

$$P = E^T(k)QE(k), \quad E(k) = \Psi\tilde{\xi}(k|k) + \Pi\Omega(k) - Y_r(k).$$

### 3 | VERIFICATIONS AND RESULTS

To investigate the effectiveness of the proposed framework, numerical simulation tests have been carried out by means of CarSim and MATLAB/Simulink. Figure 4 shows the whole



FIGURE 5 Vehicle for simulation is an 4WD E-class sedan

TABLE 3 The car parameter in the simulation

Parameter	Value	Description
$m$	1723 kg	Vehicle mass
$l_f$	1.232 m	Distance from the front axle to CG
$l_r$	1.468 m	Distance from the rear axle to CG
$C_f$	66900 N/rad	Front wheel cornering stiffness
$C_r$	62700 N/rad	Rear wheel cornering stiffness
$I_z$	4175 kg·m <sup>2</sup>	Yaw moment of inertia

simulation process in details. Figure 5 is the ego vehicle studied in the research. As is shown, vehicle model applied in CarSim is an E-class sedan like the vehicle in Figure 5 and the vehicle parameters are designed according to this kind of vehicle. Table 3 lists the constant parameters used under different conditions in the cosimulation.

Four typical scenarios are introduced to illustrate the feasibility of the aforementioned framework. Scenario A studied the car detouring for static obstacles. Scenario B and scenario C1 with different speed studied the car detouring for dynamic obstacles, respectively. Scenario C2 studied the lane changing for multiple dynamic obstacles. More details about these scenarios are described in the following.

### 3.1 | Scenario study

#### 3.1.1 | Scenario A

In this scenario, the car detouring experiments for static obstacles are conducted to verify the proposed framework. This case simulates the emergence condition that when the ego vehicle travels along the road, obstacles such as falling rocks and down-fold occur in the front suddenly. The framework to deal with this condition is: first, cameras and radars equipped on the vehicle detect the obstacle information and transmit it to VCU. Then the VCU calculate the appropriate time point using FLC,

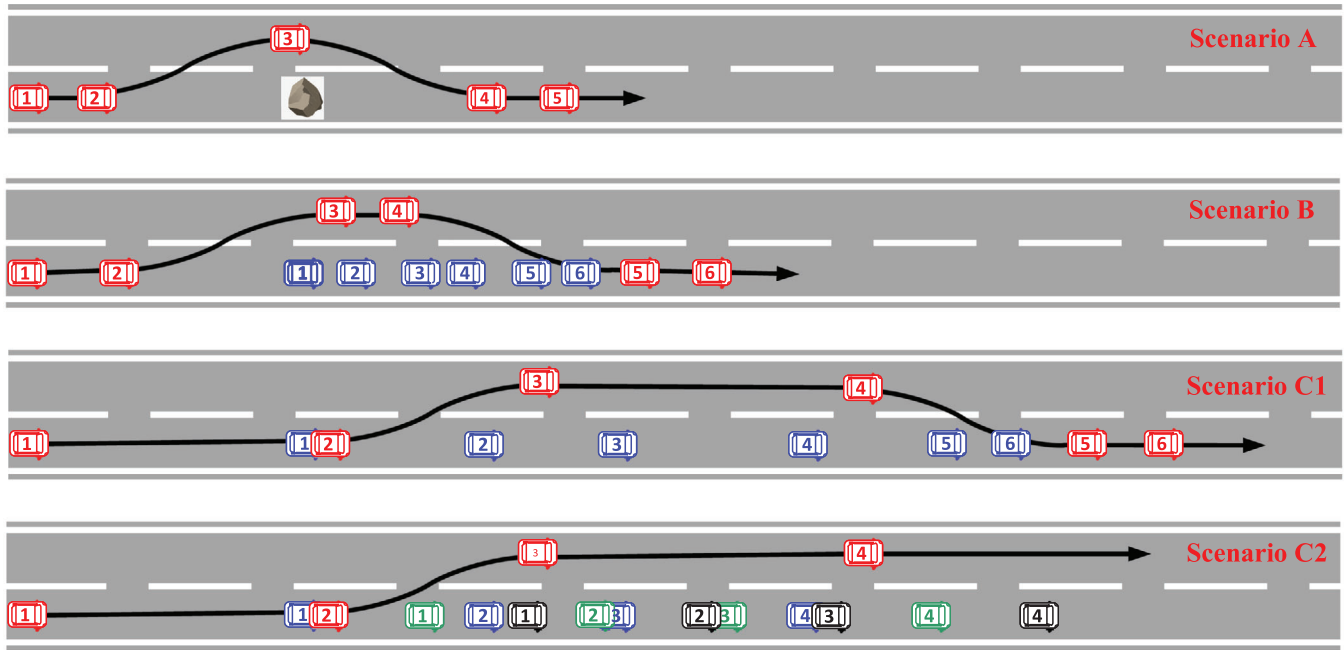


**FIGURE 6** The schematic diagram of four scenarios for changing lane

plan the obstacle avoidance path and control the actuators to track the path with the J MPC algorithm. In this scenario, the ego vehicle is driving at 60 km/h. The initial distance between the ego vehicle and the obstacle is 100 m. When the controller obtains the lane changing time point, the ego vehicle will change lane on an appropriate place. Scenario A in Figure 6 visually presents the whole car detouring process, where the ego vehicle is in red and the obstacle is a falling rock. The numbers on the vehicles represents different time to illustrate the location changing. Figures 7–10 show the vehicle state parameters in the simulation process, that is weight coefficient, SSDLC, lateral speed, lateral acceleration, yaw rate, vehicle sideslip angle, following error and so on. And these results illustrate the feasibility of the proposed framework.

### 3.1.2 | Scenario B

This scenario studies the car detouring simulation for one dynamic obstacle. The situation is similar to overtaking. The autonomous vehicle will experience two reverse lane changing, finally back to the original lane as shown in scenario B of Figure 6. The ego vehicle is in red and the heading vehicle is in blue. The numbers on the vehicles represents different time to illustrate the location changing. The ego vehicle will drive at 60 km/h, and the heading vehicle will drive at 20 km/h. The distance between them is 100 m in the beginning.

### 3.1.3 | Scenario C1

This scenario also simulates the car detouring for one dynamic with different speed. The purpose of this simulation is to study

the speed's impact on the lane changing time point. The ego vehicle will drive at 60 km/h, and the heading vehicle will drive at 40 km/h. The initial distance between them is 100 m. The schematic is shown in scenario C1 of Figure 6.

### 3.1.4 | Scenario C2

This scenario studies the lane changing for several dynamic obstacles. It simulates the typical situation that there are several moving cars in front of the ego vehicle, but the heading vehicle blocks the view. Only by means of the sensors equipped in the vehicle, the autonomous vehicle can't obtain enough information. Terminal equipment installed on the road will offer other vehicles' information. After collecting enough information, the VCU formulates the whole lane changing process, and the ego vehicle will change to the adjacent lane and drive along the lane according to the path. The visual moving process is shown in scenario C2 of Figure 6.

The ego vehicle is in red and the three moving vehicles are in blue, black, green orderly. The ego vehicle is driving at 60 km/h. These dynamic vehicles drives straight along the at 40 km/h. The initial distance between the ego vehicle and the heading vehicle is 100 m. The distance between these moving vehicles is 40 m.

## 3.2 | Results analysis

Table 4 shows that the SSDLC results using fuzzy logic control algorithm.

The velocity of the ego vehicle is set as constant while the heading vehicle drives with different velocity 0, 20 km/h,

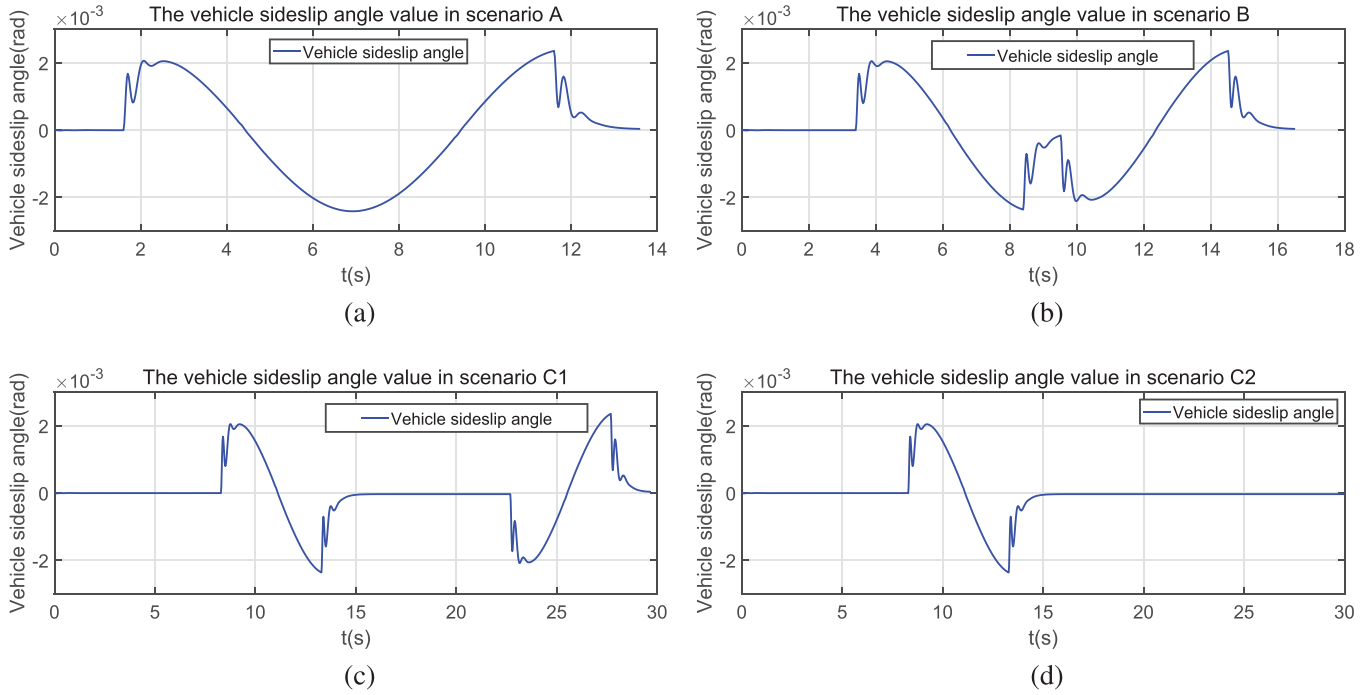


FIGURE 7 Vehicle sideslip angle responses in scenario A, B, C1, C2

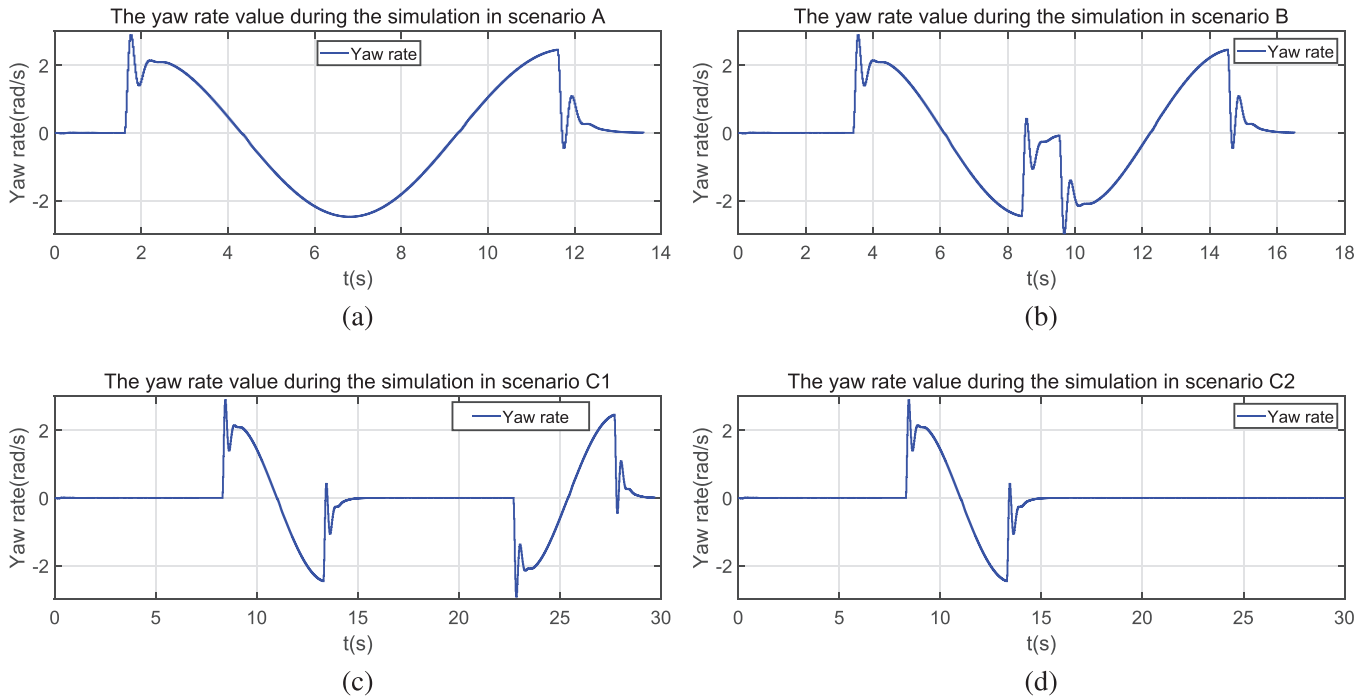


FIGURE 8 Yaw rate responses in scenario A, B, C1, C2

40 km/h. It means that the relative velocity is gradually declining. And the  $d_{change}$  mainly considering relative velocity is considerably decreasing.

The weight coefficient  $C$  also becomes less, which exactly states the weight of  $d_{refer}$  considering the velocity of the ego vehicle becomes larger, which can ensure relative safety distance

away from collisions. The reason why the weight coefficient  $C$  is less than 0.5 is that the velocity of the vehicle is high (60 km/h). In this situation, the impulse of the driving vehicle will grow large. In order to avoid risks and decrease the damage degree of traffic collisions, the safety distance related to the velocity of the ego vehicle should be as large as possible.

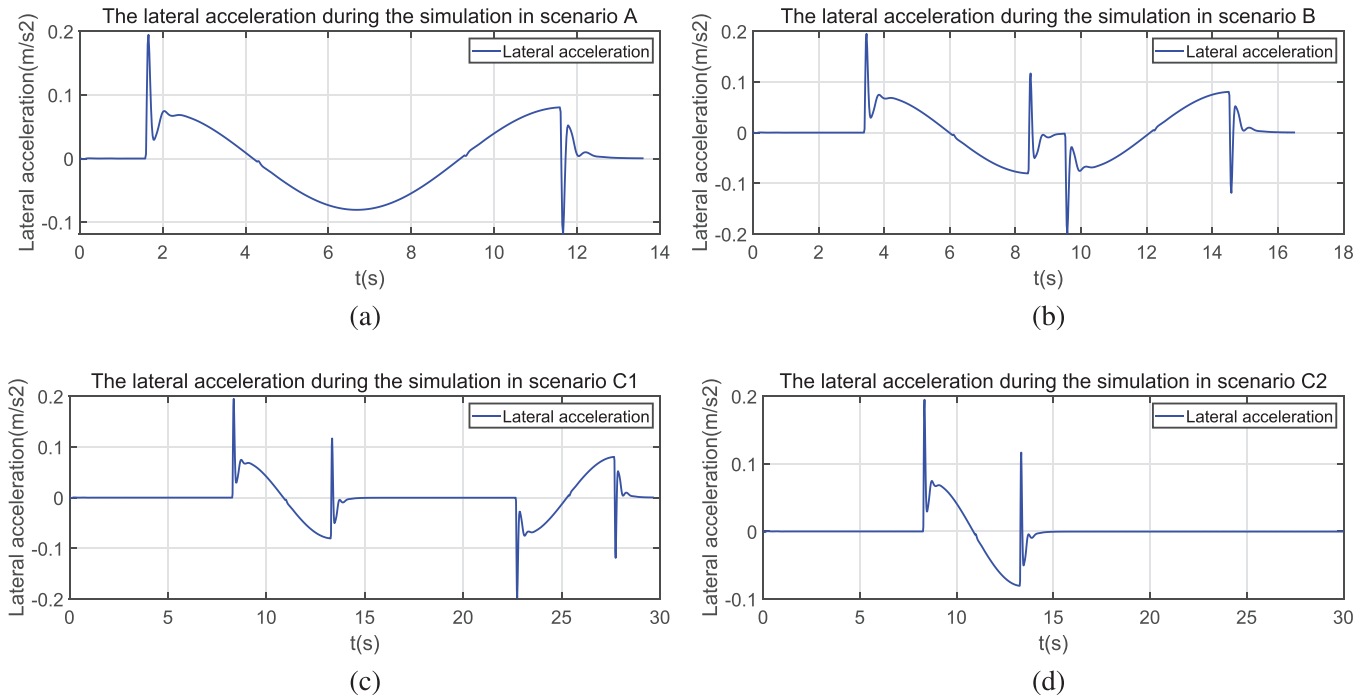


FIGURE 9 Lateral acceleration responses in scenario A, B, C1, C2

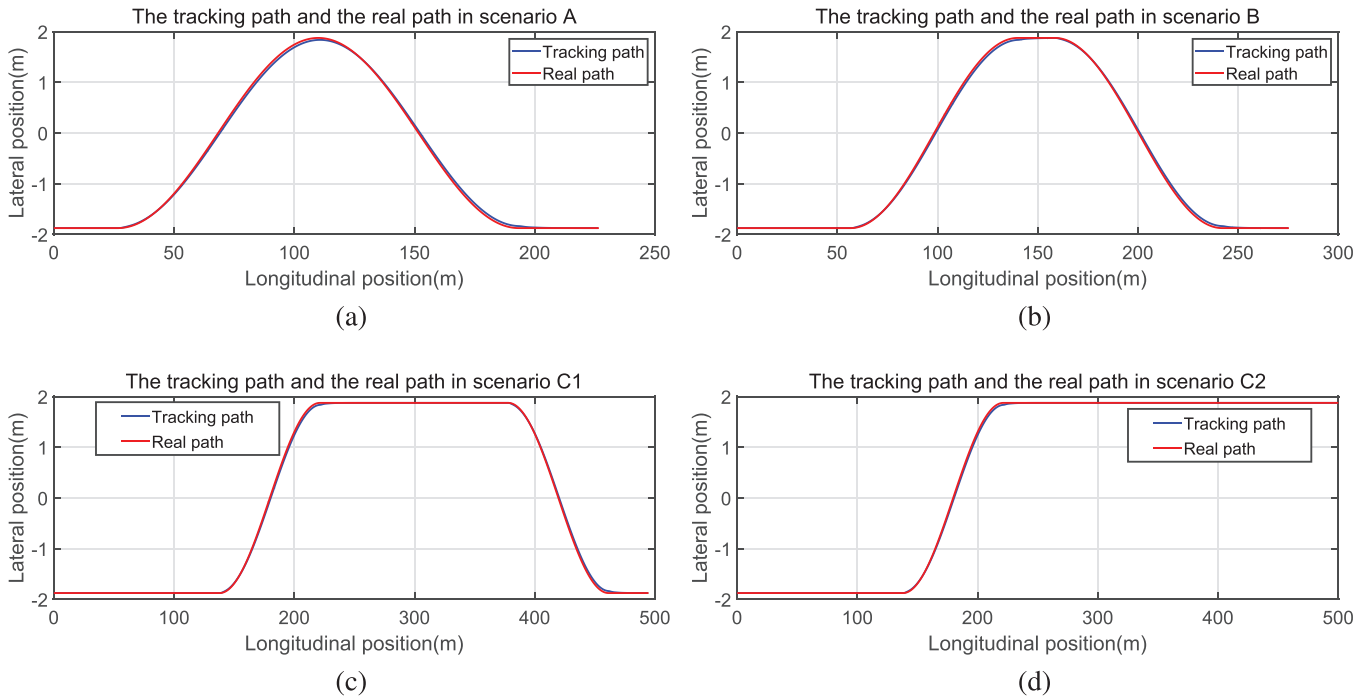


FIGURE 10 Path between tracking and real situations in scenario A, B, C1, C2

Figures 7-10 specifically shows the results of the proposed framework. From Figures 7-8, the two variables yaw rate and vehicle sideslip angle are pretty small and change smoothly during most time in all scenarios. And every time the autonomous vehicles carry out the lane changing process to track the planned path, they may experience a large variation. Although so, they

still meet the aforementioned vehicle dynamic constraints, that is vehicle sideslip angle and the yaw rate:

$$\beta \leq \tan^{-1} \left( \frac{3mg\mu}{C_c} * \frac{l_f}{l_r + l_f} \right) + l_r \frac{\dot{\phi}}{u} \approx 0.03, \quad (27)$$

**TABLE 4** The SSDLC calculation results

Parameter	Scena A	Scena B	Scena C1	Scena C2
$V_0(\text{km/h})$	60	60	60	60
$V_1(\text{km/h})$	0	20	40	40
$C$	0.397	0.3423	0.2796	0.2796
$d_{\text{change}}(\text{m})$	93	66	38	38
$d_{\text{refer}}(\text{m})$	60	60	60	60
$\text{SSDLC}(\text{m})$	73	62	54	54

$$|\dot{\phi}| = \frac{1}{mu}(F_{yf} + F_{yr}) \leq \frac{mg\mu}{mu} = \frac{g\mu}{u}$$

$$= 0.4998 \text{ rad/s} = 28.651 \text{ deg/s.} \quad (28)$$

It is quite able to ensure the yaw stability during lane changing maneuver.

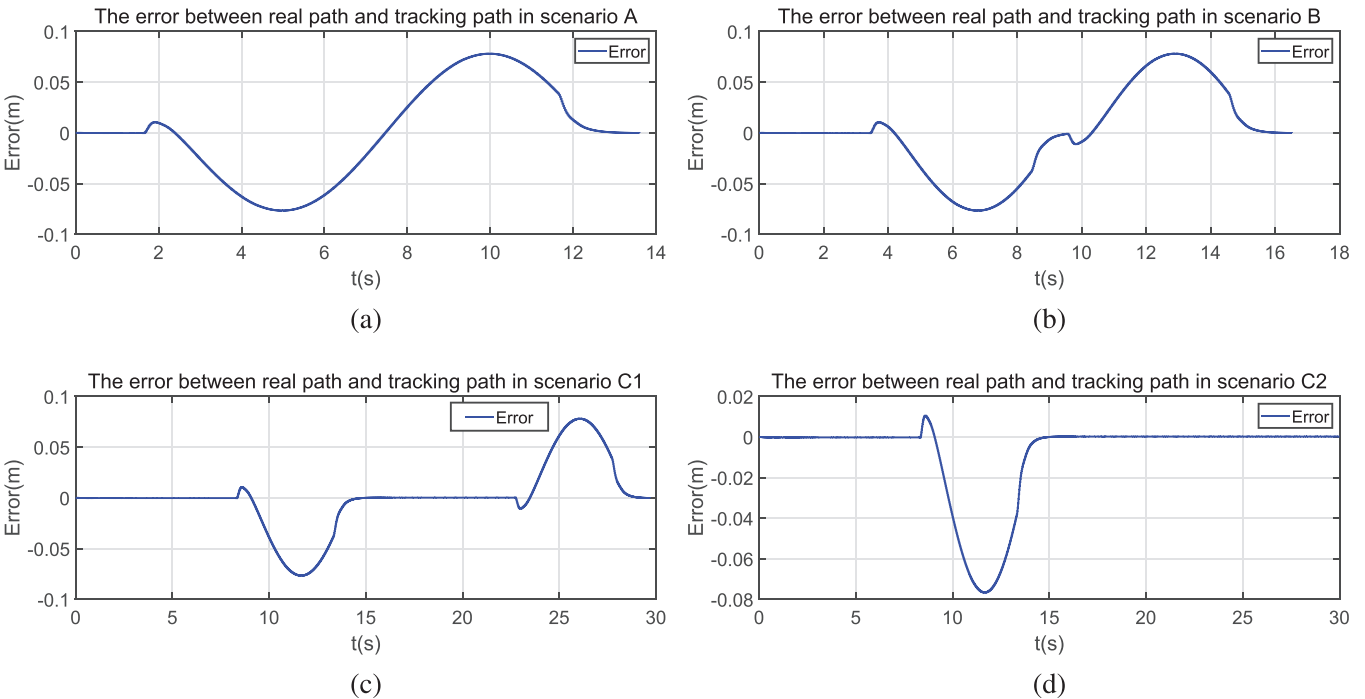
From the lateral acceleration pictures Figure 9, it can be seen that the result observes the hypothesis about vehicle model. It be supposed to be under  $0.4 \cdot g$  which is  $3.92 \text{ m/s}^2$ , and the parameter is not only under the value during the whole process, but also far less than it. It illustrates that considering the lane changing time point can leave enough room for path planning and make the planned path curvature smaller. So the lateral acceleration performs very well. It states the stability of changing lane indirectly and decrease the danger factor.

The simulation results of the real path and the tracking path are also shown in Figures 10 and 11. From these results, no matter what conditions the autonomous vehicle are in, the

maximum tracking error using JMPC is generally below  $0.1 \text{ m}$ . After some statistical calculations, the average error is  $0.0363 \text{ m}$ ,  $0.03 \text{ m}$ ,  $0.0168 \text{ m}$ ,  $0.0083 \text{ m}$ , respectively, in scenario A,B,C1,C2. The effect for tracking the straight path is generally better than that for tracking the curve path. It means those large errors happen in the curve duration while the errors are close to 0 in the straight duration. On the whole, it can be concluded that the tracking error is small due to the proposed algorithm. Apart from this, the calculation results can be convergent to the optimal results in the prescribed time. It shows that the added relaxation factor in the objective function solves the calculation issue and makes the solving process faster, and its upper value is set 10 in simulation. So these results illustrate that the JMPC can produces less tracking error and cover the complexity of vehicle dynamic problems.

## 4 | CONCLUSION

This paper studies the task of changing lanes and avoiding obstacles on structured roads. From the view of safety, studying on the lane changing time point is beneficial to ensure a smooth lane changing process. It can improve the vehicle yaw stability and the efficiency of changing lane, and it also leaves the enough room for planning the path. This paper describes an novel approach for lane changing time point. The synthesized safety distance for lane changing (SSDLC) is firstly proposed to describe the lane changing time point. It is defined as the weighted sum of traditional safety distance and lane changing safety distance. And the SSDLC is calculated by fuzzy logic control algorithm. After obtaining the appropriate lane changing time point, the whole lane changing process will begin.

**FIGURE 11** Tracking error in scenario A, B, C1, C2



Several cases in the paper demonstrate that the SSDLC can meet the safety requirements.

The joint model predictive control is proposed to follow the reference trajectory. This algorithm considers the physical saturation of actuators as well as yaw stability characteristics of the vehicle. At the same time, the JMPC adds a relaxation factor in the objective function to solve the calculation problem. Four different scenarios are conducted to verify the precision. And the maximum tracking error using JMPC is generally below 0.1m. These results show that the JMPC can produce less tracking error and cover the complexity of vehicle dynamic problems.

However, there are still some challenges. As is known, when driving on the road, different people have various driving styles, so the time it takes to change lanes for different drivers isn't same. Because the time is related to the SSDLC, the precise prediction of lane changing duration will become our further research point. Apart from this, the inherent parameters of vehicle, such as moment of inertia, may be changeable during the lane changing period. How the uncertainty of vehicle model influences the algorithm will be one of our future plans.

## ACKNOWLEDGEMENTS

This work was supported by the National Key R&D Program of China under Grant 2019YFB1600500 and National Natural Science Foundation of China under Grant U1664264.

## CONFLICT OF INTEREST

The authors have declared no conflict of interest.

## DATA AVAILABILITY STATEMENT

Data sharing is not applicable to this article as no new data were created or analyzed in this study.

## ORCID

Jiayu Fan  <https://orcid.org/0000-0002-8083-9732>

## REFERENCES

- Dixit, S., Fallah, S., Montanaro, U., et al.: Trajectory planning and tracking for autonomous overtaking: State-of-the-art and future prospects. *Annu. Rev. Control.* 45, 76–86 (2018)
- Rokonuzzaman, M., Mohajer, N., Nahavandi, S., et al.: Review and performance evaluation of path tracking controllers of autonomous vehicles. *IET Intell. Transp. Syst.* 15(5), 646–670 (2021)
- Rasekhipour, Y., Khajepour, A., Chen, S., et al.: A potential Field-Based model predictive Path-Planning controller for autonomous road vehicles. *IEEE T. Intell. Transp.* 18(5), 1255–1267 (2017)
- Zhang, Z., Wu, D., Gu, J., et al.: A Path-Planning strategy for unmanned surface vehicles based on an adaptive hybrid dynamic stepsize and target attractive Force-RRT algorithm. *J. Marine Sci. Eng.* 7(5), 132 (2019)
- Zhao, J., Knoop, V.L., Wang, M.: Two-dimensional vehicular movement modelling at intersections based on optimal control. *Transp. Res. B-Meth* 138, 1–22 (2020)
- Bichiou, Y., Rakha, H.A.: Developing an optimal intersection control system for automated connected vehicles. *IEEE T. Intell. Transp.* 20(5), 1908–1916 (2019)
- Fethi, D., Nemra, A., Louadi, K., et al.: Simultaneous localization, mapping, and path planning for unmanned vehicle using optimal control. *Adv. Mech. Eng.* 10(1), 1–25 (2018)
- Wang, R., Wang, S., Wang, Y., et al.: A paradigm for path following control of a Ribbon-Fin propelled biomimetic underwater vehicle. *IEEE T. Syst. Man. CY-S* 49(3), 482–493 (2019)
- Wang, R., Jing, H., Hu, C., et al.: Robust h-infinity path following control for autonomous ground vehicles with delay and data dropout. *IEEE T. Intell. Transp.* 17(7), 2042–2050 (2016)
- Wang, Y., Ding, H., Yuan, J., et al.: Output-feedback triple-step coordinated control for path following of autonomous ground vehicles. *Mech. Syst. Signal PR* 116, 146–159 (2019)
- Dekker, L., Marshall, J., Larsson, J.: Experiments in feedback linearized iterative learning-based path following for center-articulated industrial vehicles. *J. Field Robot.* 36(5), 955–972 (2019)
- Shan, Y., Zheng, B., Chen, L., et al.: A reinforcement Learning-Based adaptive path tracking approach for autonomous driving. *IEEE T. Veh. Technol.* 69(10), 10581–10595 (2020)
- Ji, J., Khajepour, A., Melek, W.W., et al.: Path planning and tracking for vehicle collision avoidance based on model predictive control with multi-constraints. *IEEE T. Veh. Technol.* 66(2), 952–964 (2017)
- Chen, J., Shuai, Z., Zhang, H., et al.: Path following control of autonomous Four-Wheel-Independent-Drive electric vehicles via Second-Order sliding mode and nonlinear disturbance observer techniques. *IEEE T. Ind. Electron.* 68(3), 2460–2469 (2021)
- Guo, H., Shen, C., Zhang, H., et al.: Simultaneous trajectory planning and tracking using an MPC method for Cyber-Physical systems: A case study of obstacle avoidance for an intelligent vehicle. *IEEE T. Ind. Inform.* 14(9), 4273–4283 (2018)
- Asadi, M., Fathy, M., Mahini, H., et al.: A systematic literature review of vehicle speed assistance in intelligent transportation system. *IET Intell. Transp. SY* 15(8), 973–986 (2021)
- Shim, T., Adireddy, G., Yuan, H.: Autonomous vehicle collision avoidance system using path planning and model-predictive-control-based active front steering and wheel torque control. *Proc. Inst. Mech. Eng. Part D: J. Autom. Eng.* 226(6), 767–778 (2012)
- Wu, J., Zhou, H., Liu, Z., et al.: Ride Comfort Optimization via Speed Planning and Preview Semi-Active Suspension Control for Autonomous Vehicles on Uneven Roads. *IEEE T. Veh. Technol.* 69(8), 8343–8355 (2020)
- Zhou, J., Zheng, H., Wang, J., et al.: Multiobjective optimization of Lane-Changing strategy for intelligent vehicles in complex driving environments. *IEEE T. Veh. Technol.* 69(2), 1291–1308 (2020)
- Tran, V.P., Santos, F., Garratt, M.A., et al.: Fuzzy Self-Tuning of strictly Negative-Imaginary controllers for trajectory tracking of a quadcopter unmanned aerial vehicle. *IEEE T. Ind. Electron.* 68(6), 5036–5045 (2021)
- Qun, R.: Intelligent control technology of agricultural greenhouse operation robot based on fuzzy pid path tracking algorithm. *INMATEH Agri. Eng.* 62(3), 181–190 (2020)
- Chen, J., Zhu, H., Zhang, L., et al.: Research on fuzzy control of path tracking for underwater vehicle based on genetic algorithm optimization. *Ocean Eng.* 156, 217–223 (2018)
- Dai, Y., Xue, C., Su, Q.: An integrated dynamic model and optimized fuzzy controller for path tracking of Deep-Sea mining vehicle. *J. Marine Sci. Eng.* 9(3), 249 (2021)
- Gonzalez, D., Perez, J., Milanés, V., et al.: A review of motion planning techniques for automated vehicles. *IEEE T. Intell. Transp.* 17(4), 1135–1145 (2016)
- Klancar, G., Seder, M., Blazic, S., et al.: Drivable path planning using hybrid search algorithm based on e\* and bernstein-bezier motion primitives. *IEEE T. Syst. Man Cybern.: Syst.* 51(8), 4868–4882 (2021)
- Yan, H., Yang, F., Wang, Z.: Model predictive control for unmanned tracked vehicle path following. In: 2018 International Conference on Sensing, Diagnostics, Prognostics, and Control (SDPC), pp. 101–106. IEEE, Piscataway (2018)
- Sun, W., Wang, X., Zhang, C.: A Model-Free control strategy for vehicle lateral stability with adaptive dynamic programming. *IEEE T. Ind. Electron.* 67(12), 10693–10701 (2020)

28. Cao, H., Zhao, S., Song, X., et al.: An optimal hierarchical framework of the trajectory following by convex optimisation for highly automated driving vehicles. *Vehicle Syst. Dyn.* 57(9), 1287–1317 (2019)
29. Huang, Y., Ding, H., Zhang, Y., et al.: A motion planning and tracking framework for autonomous vehicles based on artificial potential field elaborated resistance network approach. *IEEE T. Ind. Electron.* 67(2), 1376–1386 (2020)

**How to cite this article:** Fan, J., Liang, J., Tula, A.K.: A lane changing time point and path tracking framework for autonomous ground vehicle. *IET Intell. Transp. Syst.* 16, 860–874 (2022).

<https://doi.org/10.1049/itr2.12180>